**OPEN**

# Nanotopography-mediated Reverse Uptake for siRNA Delivery into Neural Stem Cells to Enhance Neuronal Differentiation

Aniruddh Solanki[1], Shreyas Shah[1], Perry T. Yin[2] & Ki-Bum Lee[1,2]

[1]Department of Chemistry and Chemical Biology, Rutgers, The State University of New Jersey, Piscataway, NJ 08854 U.S.A., [2]Department of Biomedical Engineering, Rutgers, The State University of New Jersey, Piscataway, NJ 08854 U.S.A.

RNA interference (RNAi) for controlling gene expression levels using siRNA or miRNA is emerging as an important tool in stem cell biology. However, the conventional methods used to deliver siRNA into stem cells result in significant cytotoxicity and undesirable side-effects. To this end, we have developed a nanotopography-mediated reverse uptake (NanoRU) delivery platform to demonstrate a simple and efficient technique for delivering siRNA into neural stem cells (NSCs). NanoRU consists of a self-assembled silica nanoparticle monolayer coated with extracellular matrix proteins and the desired siRNA. We use this technique to efficiently deliver siRNA against the transcription factor SOX9, which acts as a switch between neuronal and glial fate of NSCs. The knockdown of SOX9 enhanced the neuronal differentiation and decreased the glial differentiation of the NSCs. Our NanoRU platform demonstrates a novel application and the importance of nanotopography-mediated siRNA delivery into stem cells as an effective method for genetic manipulation.

One of the critical barriers to harnessing the full therapeutic potential of stem cells is the development of an easy, effective, and non-toxic methodology to control differentiation into specific cell lineages. Stem cell differentiation can be controlled by modulating key gene expression levels or signaling pathways within the cell, which has been achieved by several conventional gene delivery methods[1–5]. For example, RNA interference (RNAi) for controlling gene expression levels using siRNA or miRNA is emerging as an important tool in stem cell biology[6–8]. For the successful genetic manipulation of stem cells, the cells must typically maintain their viability for an extended period of time after single or multiple siRNA transfections, without affecting the intrinsic cellular functions. However, many of the conventional methods used to deliver siRNA into stem cells, including lipid-based transfections, cationic polyplexes, viral vectors and electroporation techniques, result in significant cytotoxicity and undesirable side-effects[9–12]. This presents a considerable challenge for achieving robust and reliable siRNA delivery into stem cells to control their differentiation into the desired cell lineages.

One of the most common methods to deliver siRNA into stem cells is solution-mediated delivery (or forward transfection), wherein the siRNA is added directly to the culture media above the seeded cells. In this approach, exogenous chemical materials are generally used to enhance cellular internalization of the siRNA. The most widely used exogenous materials include non-viral cationic lipids (such as Lipofectamine2000)[13,14] and cationic polymers (such as PEI)[4,5,12,15], which tend to condense the negatively charged siRNA to form complexes that can be readily taken up by the cell. While this approach has been found to facilitate siRNA delivery into a variety of cell types including stem cells, these exogenous materials tend to be cytotoxic and thereby need to be removed after a certain incubation period. Moreover, global gene expression studies using cDNA microarray technologies have even revealed inadvertent, nonspecific changes in gene expression within the target cells after treatment with cationic lipid and polymer-based gene delivery systems[16–18]. Such undesired side-effects can greatly exacerbate, attenuate or even mask the desired genetic change, while also compromising the ability of stem cells to proliferate, migrate and differentiate[19–22]. Therefore, there are several limitations associated with the solution-mediated delivery methods for manipulating gene expression within stem cells[23].

In an effort to address these limitations, herein we demonstrate a nanotopography-mediated reverse uptake (NanoRU) platform for delivering siRNA into neural stem cells (NSCs) in a non-toxic and highly effective

manner. The importance of nanotopography in modulating cell behavior (including adhesion, morphology, proliferation and differentiation) has become increasingly evident in recent years[24,25]. Yet, there are limited studies which report on the influence of nanotopography in facilitating cellular endocytosis, and in turn non-viral transfection[26,27]. In one such study, fibroblast and mesenchymal stem cells grown on nanotopographical patterned surfaces were shown to have enhanced endocytosis of gene plasmids, compared to unpatterned surfaces[27]. Nevertheless, while the cells were grown on the nanotopography, the gene vectors were still delivered through solution-mediated approaches (i.e. complexing with cationic polymers/lipids). Given that NSCs are known to be highly sensitive to nanotopographical and physical cues[28–30], we believe nanotopography can play a critical role in modulating siRNA uptake via substrate-mediated delivery. Our NanoRU platform was fabricated by assembling monodisperse nanoparticles on a glass substrate, which served to generate the desired nanotopographical features in the cellular microenvironment (Fig. 1). As a proof-of-concept, we studied the interaction of NSCs with different sizes of nanoparticles and identified an optimal nanoparticle size that facilitated the highest uptake of siRNA by the NSCs. To accomplish this, we assessed the efficiency of RNAi by examining the suppression of green fluorescent protein (GFP) in NSCs that were genetically modified to express GFP. Based on the GFP knockdown, we then utilized the optimized NanoRU to specifically knockdown the expression of a neural switch gene, *SOX9*, which resulted in significantly enhanced neuronal differentiation of NSCs. Thus, NanoRU relies upon the nanotopographical features of the extracellular microenvironment to deliver siRNA into NSCs, without using exogenous delivery vehicles. In particular, this novel siRNA delivery approach does not require the use of cationic transfection agents, which are generally cytotoxic to stem cells. In addition to stem cells, we further demonstrate that NanoRU can be successfully applied to deliver siRNA into various other cell lines. However, we utilize NSCs as a model cell line in order to establish NanoRU as a simple, biocompatible and efficient platform for stem cells, which are known to be much more sensitive and prone to cytotoxicity by the conventional non-viral systems used for the delivery of genetic

material[31]. In turn, we used NanoRU not only to deliver siRNA into NSCs, but also to ensure the long-term survival and differentiation of the transfected NSCs.

## Results

**Nanotopographical features determine siRNA-based gene knockdown in NSCs.** To study the effect of nanotopographical features on the efficiency of siRNA transfection and gene knockdown in the GFP-labeled NSCs, NanoRUs were fabricated by assembling monolayers of silica nanoparticles (SiNPs) ranging from 100 nm to 700 nm in diameter on bare glass substrates. The nanoparticles were assembled on the surface by centrifuging the glass substrates in a solution of positively-charged SiNPs[32]. This size-dependent study is critical because the nanotopographical features of the extracellular microenvironment have been shown to affect the adhesion and growth of stem cells, which in turn can influence the substrate-mediated delivery of genetic materials into stem cells[25,26,33,34]. For our initial studies, siRNA targeting GFP was selected to assess the efficiency of siRNA delivery and GFP knockdown in the NSCs. After nanoparticle assembly, the NanoRUs were coated with a solution of laminin (10 μg/mL) and siRNA molecules (1 μM) against GFP. Laminin is a well-established extracellular matrix (ECM) protein that binds to the integrin receptors on the surface of the NSCs, and is an essential ECM component for the adhesion, growth, and differentiation of NSCs[35,36]. Negatively-charged siRNA molecules and laminin condensed together on the positively-charged SiNPs. After 4 h, the solution was removed and NSCs were then seeded on these NanoRUs (Fig. 2a). After 72 h, the NanoRUs were imaged using a fluorescence microscope and the knockdown of GFP in the NSCs was quantified. Interestingly, we observed a size-dependent knockdown of GFP in the NSCs, wherein the 100 nm SiNPs showed the highest knockdown and the 700 nm particles showed the lowest knockdown (Fig. 2b). These results were normalized with the fluorescence from NSCs on control substrates having no SiNPs (i.e. absence of nanotopography). The control substrates (without the SiNP monolayer) had a positively-charged surface, which was prepared by functionalizing glass substrates with
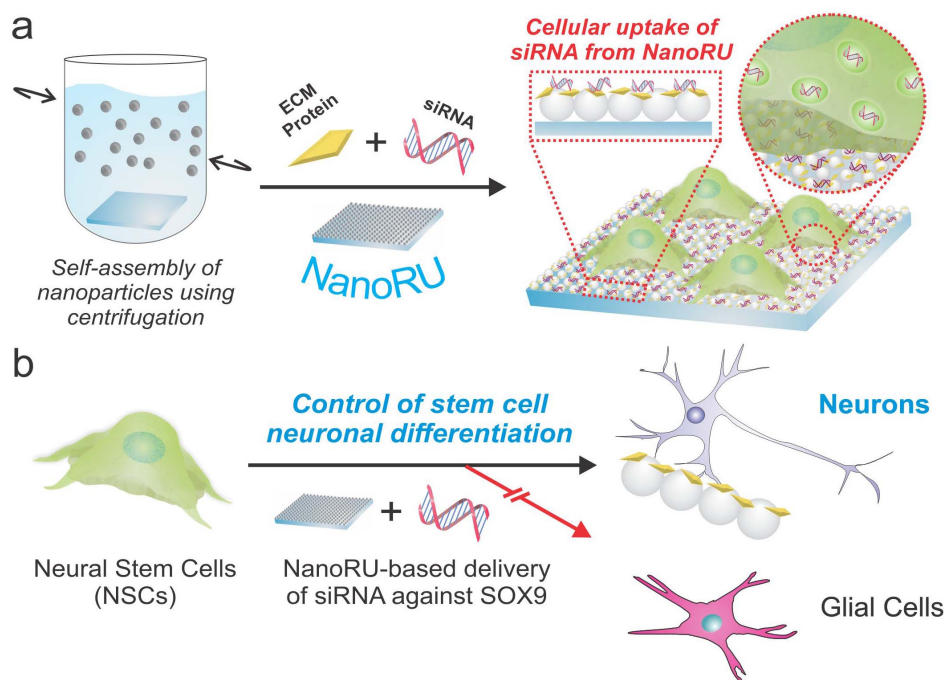


**Figure 1 | Schematic diagram depicting the application of NanoRU.** (a) The cellular uptake of siRNA into NSCs from NanoRU coated with ECM protein and siRNA molecules. (b) The delivery of siRNA against the SOX9 transcription factor using NanoRU to promote neuronal differentiation of NSCs.
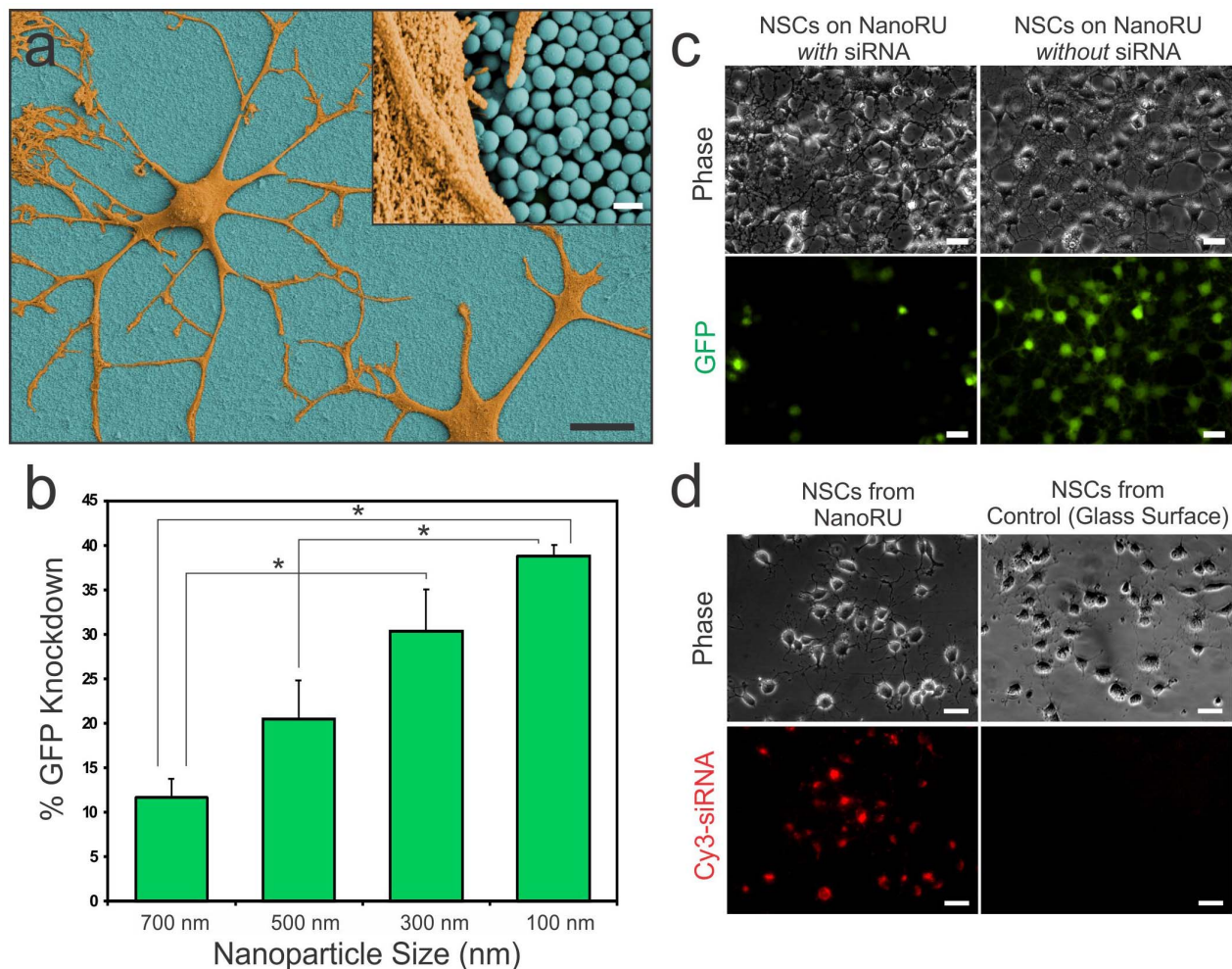
**Figure 2 | Characterizing cellular uptake of siRNA from NanoRU.** (a) Scanning electron microscopy (SEM) image of NSCs on NanoRU. The NSCs (orange) and the NanoRU (blue) in the SEM image have been pseudocolored to enhance the contrast. Scale bar: 10 μm. Inset: Magnified view. Scale bar: 500 nm. (b) Quantitative comparison of the percentage of GFP knockdown in NSCs on NanoRU containing nanoparticles ranging in size from 100–700 nm. Analysis of variance (ANOVA) was used for evaluating the statistical significance of GFP knockdown (* = P < 0.05). (c) Phase and fluorescence images of NSCs on NanoRU with and without GFP siRNA. Scale bars: 20 μm. (d) Left column: Phase contrast and fluorescence image of NSCs grown on NanoRU coated with Silencer® Cy3-labeled control siRNA, and then reseeded in a 24-well plate. Right column: Phase image and fluorescence image of NSCs grown on a control substrate (bare glass surface without nanofeatures) coated with Silencer® Cy3-labeled control siRNA, and then re-seeded into a 24-well plate. Scale bars: 20 μm.

self-assembled monolayers (SAMs) of 3-Aminopropyltrimethoxy silane (APTES) and subsequently coating them with the same concentrations of siRNA and laminin. To further substantiate that the siRNA uptake and gene knockdown was due to the differences in the nanopotographical features and not due to the differences in the amount of siRNA bound, we performed the Picogreen® assay to quantify the amount of siRNA bound to NanoRUs. From the Picogreen® assay, we confirmed that the amount of siRNA bound to all the NanoRUs (100–700 nm and control substrates) was around 30%, thus confirming that the siRNA uptake and gene knockdown was indeed due to the nanotopographical features on the NanoRUs. Given that the NanoRU fabricated using 100 nm SiNPs resulted in maximum GFP knockdown, all of the subsequent experiments were carried out using NanoRU with 100 nm SiNPs.

**NanoRU delivers only siRNA into NSCs and not SiNPs.** Another important aspect that needed to be investigated was whether the SiNPs were being taken up along with the siRNA. To this end, we used SiNPs labeled with Alexa-Fluor® 594 dye to generate nanotopographical features on glass substrates. We then deposited

siRNA against GFP on the dye-labeled NanoRUs. After 36 h of incubation, the NSCs were detached gently from the NanoRU using the enzyme Accutase®, and regrown in a 24-well plate. We did not observe any fluorescence (from the dye-labeled SiNPs) within the transfected NSCs. However, we observed a clear GFP knockdown due to the siRNA delivered into the NSCs (Fig. 2c). We further used transmission electron microscopy (TEM) to confirm that the SiNPs are not taken up by the NSCs (Fig. S1). We then confirmed the uptake and localization of siRNA from NanoRU using the *Silencer*® Cy3-labeled negative control siRNA (Ambion), which showed remarkably higher fluorescence compared to the control substrates (Fig. 2d). This experimental data clearly indicates that the stem cells take up only siRNAs, and not SiNPs. We believe that this unique feature, where only the siRNA is taken up by the NSCs, makes NanoRU particularly advantageous over conventional transfection methods for stem cell research.

We further sought to investigate the mechanism involved in the uptake of siRNA from NanoRU. ECM proteins such as laminin, fibronectin and collagen pre-adsorbed on surfaces have been previously implicated in enhancing gene delivery through

endocytosis[33,37,38]. Gene delivery in such systems depended primarily upon caveolae- than clathrin-mediated endocytosis[37]. Caveolae-mediated endocytosis is known to be more efficient as it is able to circumvent the degradative lysosomal pathway[39]. To confirm if the dominant endocytic pathway involved in the uptake of siRNA by the NSCs cultured on NanoRU was indeed caveolae-mediated endocytosis, we treated the NSCs with 100 μM of indomethacin (10 min), a specific inhibitor of caveolae-mediated endocytosis. We also treated the NSCs with a mixture of 10 mM sodium azide and 5 mM 2-Deoxy-D-glucose (10 min) as this mixture inhibits all endocytotic pathways within the NSCs. After 72 h, we observed a 13% knockdown of GFP in NSCs treated with Indomethacin and a 7% knockdown in NSCs treated with the mixture of sodium azide and 2-Deoxy-D-glucose, which was significantly lower than the 40% knockdown observed in untreated NSCs (Fig. S2). Collectively, our results imply that the uptake of siRNA using NanoRU relies mainly on the caveolae-mediated endocytosis. However, there may be multiple pathways involved in the uptake of siRNA from NanoRU, which are currently under investigation in our lab.

**Controlling neuronal differentiation of NSCs using NanoRU.** Having demonstrated the efficiency of NanoRU by delivering siRNA against GFP, we focused on using NanoRU to enhance the neuronal differentiation of NSCs by suppressing the expression of a specific protein or gene. We used NanoRU to deliver siRNA against SOX9 (siSOX9), a well-established transcription factor which acts as a switch between neuronal and glial differentiation[40]. When the SOX9 gene is "turned on," a higher percentage of NSCs differentiate into astrocytes (glial cells), and when "turned off," a higher percentage of NSCs differentiate into neurons[40–42]. To this end, we used NanoRU for the delivery of siRNA to "turn off" SOX9, wherein we coated NanoRU with laminin and siSOX9 following the experimental protocols we had established for knocking down GFP. The NSCs were then cultured on NanoRU. After 72 h, the knockdown of SOX9 was analyzed using RT-PCR and a significant decrease in the mRNA levels of SOX9 was observed (Fig. 3a). The NSCs were grown and differentiated on the NanoRU coated with the siSOX9 for 7 days. We then used RT-PCR to examine the expression levels of key neural markers (Fig. 3a). A remarkable decrease in the expression of the glial marker, glial fibrillary acidic protein (GFAP), and an increase in the expression of the neuronal marker, β-III tubulin (TuJ1), was observed. No significant change was found in the expression of the oligodendrocyte marker, myelin-binding protein (MBP). We further confirmed and quantified our results by immunostaining for neuronal and astrocyte markers (Fig. 3b and 3c). Compared to control substrates (substrates having no SiNPs), a remarkably higher percentage of NSCs differentiated into neurons on NanoRU coated with siSOX9 (Figure 3b). As expected, the number of astrocytes considerably decreased when SOX9 was knocked down. Neuronal differentiation was further confirmed by studying the co-localization of two different neuronal markers, TuJ1 and microtubule-associated protein 2 (MAP2) (Fig. S3).
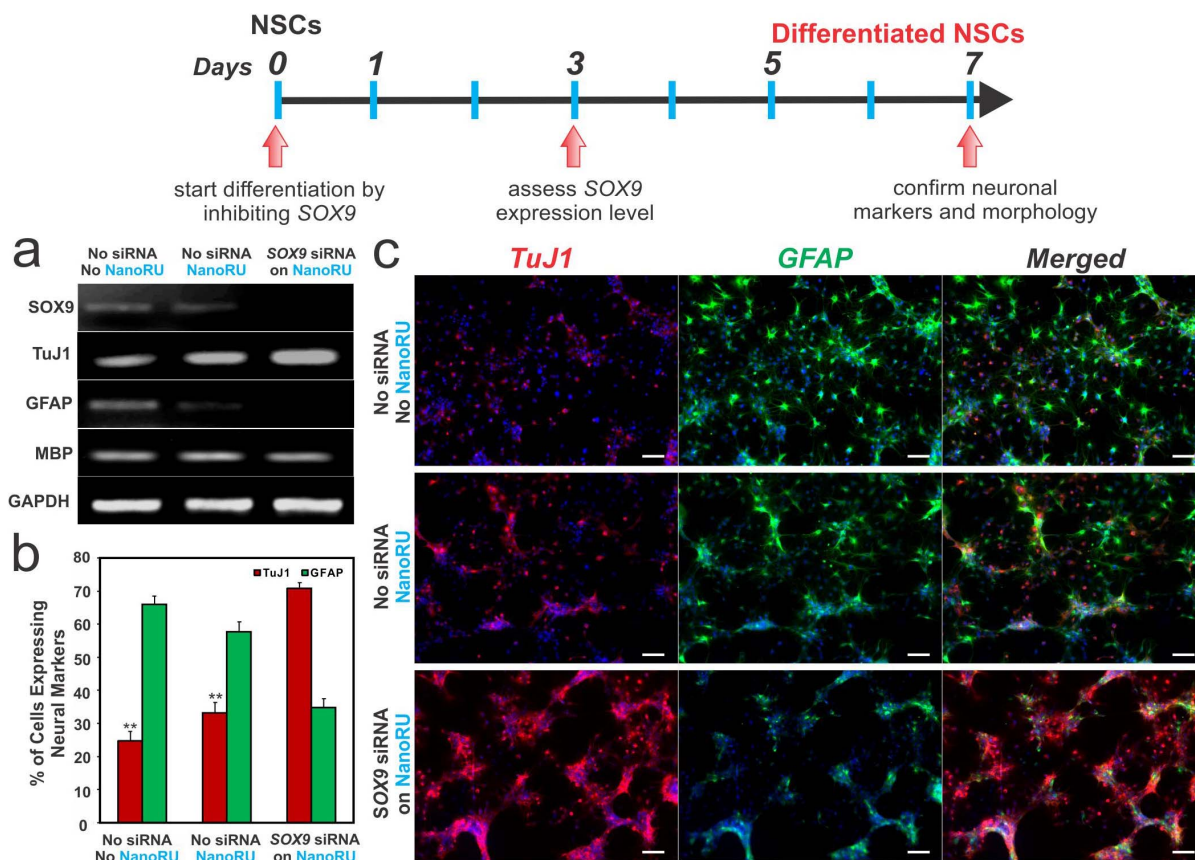


**Figure 3** | **NSC differentiation on NanoRU coated with SOX9 siRNA (siSOX9).** (a) RT-PCR analysis reveals differences in transcript levels for SOX9 and differentiation markers for neurons (TuJ1), astrocytes (GFAP) and oligodendrocytes (MBP) in the presence or absence of siSOX9 and/or NanoRU. (b) Quantitative comparison of the percentage of cells expressing TuJ1 and GFAP. Student's unpaired t-test was used for evaluating the statistical significance for cells stained for TuJ1, compared to the siSOX9 on NanoRU condition (** = P < 0.001). (c) Fluorescence images of cells stained for the nucleus (blue), the neuronal marker TuJ1 (red, left column), the astrocyte marker GFAP (green, middle column) and merged (last column) show the extent of differentiation of NSCs grown on: no NanoRU nor siSOX9 coating (top row), NanoRU without siSOX9 coating (middle row), and NanoRU with siSOX9 coating (bottom row). Scale bars: 50 μm.

**NanoRU for delivering siRNA into other mammalian cells and miRNA into NSCs.** After successfully demonstrating the proficiency of NanoRU for delivering siRNA into stem cells, we sought to explore the potential of using NanoRU as a platform for delivering siRNA into other mammalian cell lines. To this end, NanoRU was used to deliver Silencer® Cy3-labeled negative control siRNA into other mammalian cells such as astrocytes, brain cancer cells (U87-VIII), and breast cancer cells (SUM159). The cells were detached from NanoRU after 36 h, replated in 24 well plates, and then imaged for siRNA uptake (Fig. 4a and S4). All of the cell lines showed the uptake of the dye-labeled siRNA from NanoRU, indicating that our technique is efficient and applicable to normal cells, cancer cells, as well as stem cells. Additionally, NanoRU can be easily extended to deliver miRNA, consisting of a larger number of nucleotide base pairs. We successfully delivered the Cy3-dye labeled Pre-miR® negative control (Ambion) using the same protocol that we used for delivering siRNA. The NSCs cultured on NanoRU coated with laminin and miRNA took up the miRNA in a highly efficient manner (Fig. S5).

**NanoRU does not damage cell membranes and is non-toxic.** One of the biggest advantages of NanoRU is its biocompatibility and the fact that the transfection begins as soon as the cells are cultured on NanoRU, with the highest transfection observed at 36 h (Fig. S6). On the other hand, most standard solution-mediated transfection protocols using cationic lipids and polymers require a wait period of at least 12–24 h before the cells can be transfected in order to minimize their toxicity. In addition, the serum proteins in the culture media are known to decrease the transfection efficiency due to the non-specific interaction of serum proteins with the delivery constructs[43]. We compared the cytotoxicity of NanoRU with a well-established lipid-based cationic transfection agent, Lipofectamine 2000® (Life Technologies) using the negative

control siRNA in three different cell lines: SUM159, U87VIII and NSCs. The cytotoxic results were analyzed using a standard cell proliferation assay (MTS assay). Interestingly, we found that Lipofectamine 2000®, while less toxic towards cancer cells, was extremely cytotoxic (using manufacturer's recommended transfection condition) towards NSCs, which led to 95% cell death within 48 h of being transfected with the negative control siRNA (Fig. 4b). NanoRU, on the other hand, was seen to be biocompatible with a minimal decrease in cell viability for all the cell lines tested. Moreover, we believe NanoRU does not cause any physical damage to the cell membranes as the NSCs showed high cellular viability and enhanced neuronal differentiation on NanoRU after an extensive period of 7 days. Hence, NanoRU can be especially useful for controlling NSC differentiation, a process which requires the NSCs to survive for more than seven days *in vitro*.

## Discussion

While most studies have aimed to improve the efficiency of siRNA delivery by trying to improve the delivery vehicle, modulating the cellular microenvironment is an attractive means to achieve superior transfection efficiency. In turn, increasing attention has been given to substrate-mediated delivery (or reverse transfection), wherein the cells directly uptake the gene vector from the underlying substrate[44–47]. This approach has been found to result in greater internalization and functional expression of the gene vectors (i.e. DNA plasmids) compared to forward transfection[45]. However, up to now, these approaches have relied on using cationic lipids or polymers to complex the gene vector prior to immobilizing on the substrate, in turn suffering from issues with cytotoxicity and nonspecific changes in gene expression. Substrate-mediated methods which do not utilize cationic materials have also been successful at delivering biomolecules into cells[48–51]. However, the cell survival on such substrates for extended periods, which is especially important for
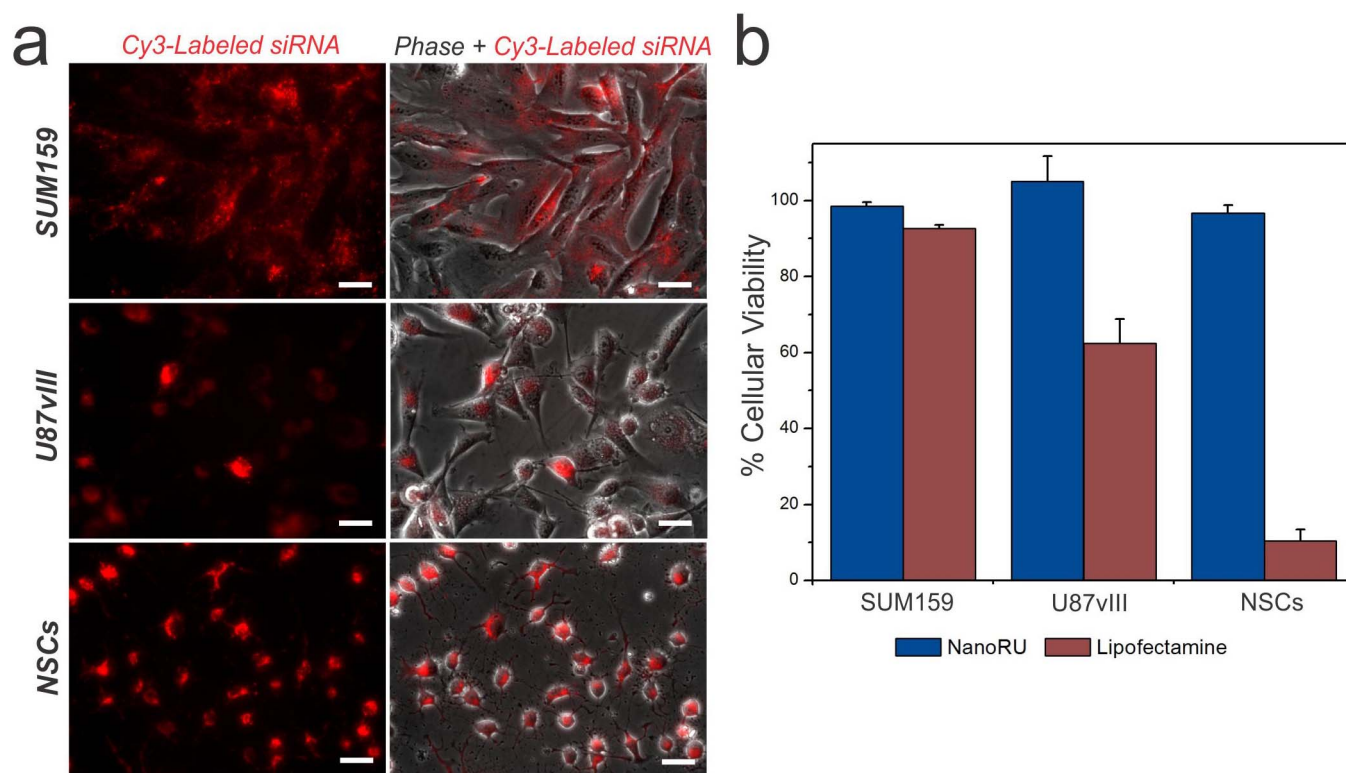


**Figure 4 | Cellular uptake of siRNA and cellular viability in different cell types.** (a) Fluorescence (left column) and merged phase images (right column) of the Silencer® Cy3-labeled negative control siRNA from NanoRU in three cell lines: SUM159 (breast cancer cells), U87vIII (brain cancer cells) and rat NSCs (neural stem cells). Scale bars: 20 μm. (b) MTS cellular viability of SUM159, U87vIII and NSCs grown on NanoRU.

**Table 1 | Primers used in PCR analysis**

| Gene | F Primer | R Primer | Size (bp) |
|---|---|---|---|
| GAPDH | 5′-ATGACTCTACCCACGGCAAG-3′ | 5′-GGAAGATGGTGATGGGTTTC-3′ | 87 |
| GFAP | 5′-GAGAGAGATTCGCACTCAGTA-3′ | 5′-TGAGGTCTGCAAACTTGGAC-3′ | 89 |
| MBP | 5′-CACAAGAACTACCCACTACGG-3′ | 5′-GGGTGTACGAGGTGTCACAA-3′ | 103 |
| SOX9 | 5′-AGGAAGCTGGCAGACCAGTACC-3′ | 5′-TCTCTTCTCGCTCTCGTTCA-3′ | 96 |
| TUJ1 | 5′-ACTTTATCTTCGGTCAGAGTG-3′ | 5′-CTCACGACATCCAGGACTGA-3′ | 97 |

advancing stem cell therapies, is critically important and less explored. Our approach addresses the necessity to develop a non-toxic and efficient strategy for delivering siRNA into stem cells to control gene expression levels, such that we can maintain the biological functions of stem cells for extended periods of time and efficiently control their differentiation into specific cell types.

We have developed a novel nanotopography-mediated reverse uptake (NanoRU) platform, for the genetic manipulation of NSCs in a highly effective manner. This platform was employed to control the neuronal differentiation of stem cells by using nanotopographical features to deliver siRNAs inside cells. We believe NanoRU and its application can significantly complement recent advances in research efforts to control stem cell differentiation based on physical cues such as patterns and bioactive scaffolds of ECM materials. Even though we have only explored proof-of-concept experiments involving genetic manipulation and differentiation of NSCs, we expect that NanoRU can be extended, with straightforward modifications of the aforementioned protocols, to a wide range of nanomaterials and biomolecules (e.g. miRNA, proteins, and small molecules). Finally, we believe NanoRU is a valuable platform which will complement conventional genetic manipulation tools in cell biology. For example, one of the key aspects behind stem cell-based therapies for many devastating diseases is to transplant stem cells or differentiated stem cells at the site of injury, after genetically manipulating them. The exogenous delivery vehicles used for siRNA delivery would be present within the stem cells and could trigger a strong immune response or tumor formation after stem cell transplantation. Therefore, our NanoRU-based siRNA delivery can potentially help overcome one of the critical barriers in stem cell-based tissue engineering.

## Methods

**NanoRU preparation.** Cover glass (Number 1, 22 mm × 22 mm; VWR) was cut equally into smaller pieces (18 mm × 6 mm) and sonicated in Nanopure water (18.2 mOhm) for 10 mins and then cleaned in piranha solution (a 3 : 1 mixture of sulphuric acid and hydrogen peroxide) for 10 min (Caution: Piranha solution is extremely corrosive). The glass coverslips were then washed again in Nanopure water (18.2 Mohm) and dried under a stream of pure nitrogen. To generate films of nanotopographical features, positively-charged (amine-terminated) silicon oxide nanoparticles (SiNPs, Corpuscular Inc) of different sizes were utilized. The washed cover slips were centrifuged at 2000 RPM for 2 min in a 2 mL eppendorf tube containing 25 mg/mL of the SiNP solution. The sizes used were 50 nm, 100 nm, 300 nm, 500 nm and 700 nm. The substrates were then washed with Nanopure water and dried under a stream of pure nitrogen. For functionalization with (3-aminopropyl)triethoxysilane (APTES), the washed glass cover slips were left in a beaker containing 1% APTES solution in pure ethanol for 2 h. The cover slips were then rinsed thoroughly with ethanol and dried under nitrogen. They were then baked at 100°C in an oven for 10 min.

**Coating NanoRU with laminin and siRNA.** The NanoRUs were then coated with siRNA and laminin, both of which are negatively charged at in phosphate buffer saline (PBS, pH 7.4; Life Technologies). In a culture hood, NanoRUs were coated with a 10 μg/mL solution of laminin containing 100 pmoles of the desired siRNA (against GFP or *SOX9*). The GFP siRNA sequence was: Antisense – 5′-CCAACGACAUCAGCGACUAUU-3′, Sense – 3′-UUGGUUGCUGUAGUCGCUGAU-5′. The *SOX9* siRNA sequence was Antisense – 5′-AACGAGAGCGAGAAGAGACCC-3′, Sense – 3′-TTGCUCUCGCUCUUCUCUGGG-5′. The solution was left on top of the NanoRUs for 3 h, and then simply removed by dipping the films once in sterile PBS. The negatively charged laminin and siRNA molecules simply condense on the positively charged NanoRU. The coated NanoRUs were then put into 12 well plates and 1 mL suspensions of NSCs were seeded with density of 1.25 × 10^5 NSCs/ml of Millitrace media (Millipore) in the absence of growth factors such as basic fibroblast growth factor (bFGF). The NSCs were maintained in a humidified atmosphere at 37°C and 5% CO_2. After 12 h, the films were transferred to new well plates to prevent

non-specific attachment of the floating NSCs. The media was then changed every other day until Day 7. On Day 7, the cells were either fixed for immunocytochemistry or lysed for PCR analysis.

**Rat neural stem cell (NSC) culture and differentiation.** Rat neural stem cell line (Millipore) were purchased and routinely expanded according to the manufacture's protocol. The NSCs were maintained in laminin (Sigma, 20 μg/ml) coated culture dishes precoated with poly-L-lysine (10 μg/ml) in Millitrace media (Millipore) supplemented with the antibiotics, penicillin and streptomycin (Life Technologies), in the presence of basic fibroblast growth factor (bFGF-2, 20 ng/ml, Millipore). All of the cells were maintained at 37°C in a humidified atmosphere of 5% CO_2. For consistency, the experiments were carried out on cells between passages 2 and 5. Neural differentiation was initiated by changing the medium to basal medium (without bFGF-2) on the NanoRUs coated with laminin and siRNA. The cells were allowed to differentiate for 7 days with the basal medium in each being exchanged every other day.

**Culturing U87-EGFRvIII, SUM159, and astrocytes.** For each of the three non-stem cell lines, experiments were carried out on cells between passages 2 and 10. The NanoRU, coated with Silencer Cy3-labeled negative control siRNA, were put into wells of a 12-well plate and each well containing the substrate was seeded with 80,000 cells. After 24 h, the substrates were moved into a new 12 well plate. The media components for U87-EGFRvIII cell line include DMEM (Dulbecco's modified Eagle's medium) with high glucose (Invitrogen), 10% Fetal Bovine Serum (FBS), 1% streptomycin-penicillin, 1% glutamax (Invitrogen), and the selection marker, hygromycin B (30μg/ml). The media components for SUM159 cell line include Ham's F12 with insulin (5.0 μg/mL), hydrocortisone (1.0 μg/mL), 10 mM HEPES buffer, 5% Fetal Bovine Serum (FBS), 1% streptomycin-penicillin. The media components for the Astrocytes cell line DMEM with high glucose (Invitrogen), 10% Fetal Bovine Serum (FBS), 1% streptomycin-penicillin, 1% glutamax (Invitrogen).

**Cell viability assays.** Cell viability of the above cell lines on NanoRU was compared with Lipofectamine 2000® (Life Technologies) for delivering *Silencer®* negative control siRNA (Ambion). The percentage of viable cells was determined by MTS assay following standard protocols described by the manufacturer. All experiments were conducted in triplicate and averaged. The quantification of cytotoxicity was done using MTS assay after incubating cells in the presence of the manufacturer's recommended concentration of Lipofectamine 2000®. The data is represented as formazan absorbance at 490 nm, considering the control (untreated) cells as 100% viable.

**Immunocytochemistry.** To investigate the extent of neuronal differentiation, at Day 6, the basal medium was removed and the cells fixed for 15 minutes in Formalin solution (Sigma) followed by two PBS washes. Cells were permeabilized with 0.1% Triton X-100 in PBS for 10 minutes and non- specific binding was blocked with 5% normal goat serum (NGS, Life Technologies) in PBS for 1 hour at room temperature. To study the extent of neuronal differentiation the primary mouse antibody against TuJ1 (1 : 500, Covance) and primary rabbit antibody against MAP2 (1 : 100, Cell Signaling) was used and for glial differentiation the primary rabbit antibody against GFAP (1 : 300, Dako) was used. The fixed samples were incubated overnight at 4°C in solutions of primary antibodies in PBS containing 10% NGS. After washing three times with PBS, the samples were incubated for 1 h at room temperature in solution of anti-mouse secondary antibody labeled with Alexa-Fluor® 647 and anti-rabbit secondary antibody labeled with Alexa-Fluor® 546 (1 : 200, Life Technologies), Hoechst 33342(1 : 500, Life Technologies) in PBS containing 10% NGS to observe neuronal and glial differentiation. After washing the samples thrice with PBS, the substrates were mounted on glass slides using ProLong® Gold antifade (Life Technologies) to minimize quenching by gold. The mounted samples were imaged using Nikon TE2000 Fluorescence Microscope. ImageJ (NIH) was used for comparative analysis and quantifying the cells expression TuJ1 and GFAP.

**PCR analysis.** Total RNA was extracted using Trizol Reagent (Life Technologies) and the mRNA expression level of GFAP, MBP, SOX9 and TUJ1 were analyzed using Reverse Transcriptase PCR (RT-PCR) and quantitative PCR (qPCR). Specifically, cDNA was generated from 1 μg of total RNA using the Superscript III First-Strand Synthesis System (Life Technologies). Analysis of mRNA was then accomplished using primers specific to each of the target mRNAs. RT-PCR reactions were performed in a Mastercycler Ep gradient S (Eppendorf) and images were captured using a Gel Logic 112 (Carestream) imaging system. qPCR reactions were performed using SYBR Green PCR Master Mix (Applied Biosystems) in a StepOnePlus Real-

Time PCR System (Applied Biosystems) and the resulting $C_t$ values were normalized to GAPDH. Standard cycling conditions were used for all reactions with a melting temperature of 60°C. Primers are listed below (see Table 1).

1. Ferreira, L., Karp, J. M., Nobre, L. & Langer, R. New opportunities: The use of Nanotechnologies to manipulate and track stem cells. *Cell Stem Cell* **3**, 136–146 (2008).

2. Kumar, S., Chanda, D. & Ponnazhagan, S. Therapeutic potential of genetically modified mesenchymal stem cells. *Gene Ther.* **15**, 711–715 (2008).

3. Green, J. J. *et al.* Nanoparticles for Gene Transfer to Human Embryonic Stem Cell Colonies. *Nano Letters* **8**, 3126–3130 (2008).

4. Yang, F. *et al.* Genetic engineering of human stem cells for enhanced angiogenesis using biodegradable polymeric nanoparticles. *Proc. Natl. Acad. Sci. USA* **107**, 3317–3322 (2010).

5. Zoldan, J. *et al.* Directing human embryonic stem cell differentiation by non-viral delivery of siRNA in 3D culture. *Biomaterials* **32**, 7793–7800 (2011).

6. Ding, L. & Buchholz, F. RNAi in embryonic stem cells. *Stem Cell Rev.* **2**, 11–18 (2006).

7. Heidersbach, A., Gaspar-Maia, A., McManus, M. T. & Ramalho-Santos, M. RNA interference in embryonic stem cells and the prospects for future therapies. *Gene Ther.* **13**, 478–486 (2006).

8. Yau, W. W. Y., Rujitanaroj, P. O., Lam, L. & Chew, S. Y. Directing stem cell fate by controlled RNA interference. *Biomaterials* **33**, 2608–2628 (2012).

9. Geng, T., Zhan, Y. H., Wang, J. & Lu, C. Transfection of cells using flow-through electroporation based on constant voltage. *Nature Protoc.* **6**, 1192–1208 (2011).

10. Kim, J. E., Shin, J. Y. & Cho, M. H. Magnetic nanoparticles: an update of application for drug delivery and possible toxic effects. *Arch. Toxicol.* **86**, 685–700 (2012).

11. van Gaal, E. V. B. *et al.* How to screen non-viral gene delivery systems in vitro? *J. Control. Release* **154**, 218–232 (2011).

12. Merdan, T., Kopecek, J. & Kissel, T. Prospects for cationic polymers in gene and oligonucleotide therapy against cancer. *Adv. Drug Deliver. Rev.* **54**, 715–758 (2002).

13. Rosner, M. *et al.* Efficient siRNA-mediated prolonged gene silencing in human amniotic fluid stem cells. *Nature Protoc.* **5**, 1081–1095 (2010).

14. McMahon, K. M. *et al.* Biomimetic High Density Lipoprotein Nanoparticles For Nucleic Acid Delivery. *Nano Lett.* **11**, 1208–1214 (2011).

15. Tseng, S. J. & Tang, S. C. Development of poly(amino ester glycol urethane)/siRNA polyplexes for gene silencing. *Bioconjugate Chem.* **18**, 1383–1390 (2007).

16. Omidi, Y., Barar, J. & Akhtar, S. Toxicogenomics of cationic lipid-based vectors for gene therapy: impact of microarray technology. *Curr Drug Deliv* **2**, 429–41 (2005).

17. Akhtar, S. & Benter, I. Toxicogenomics of non-viral drug delivery systems for RNAi: potential impact on siRNA-mediated gene silencing activity and specificity. *Adv Drug Deliv Rev* **59**, 164–82 (2007).

18. Omidi, Y. *et al.* Microarray analysis of the toxicogenomics and the genotoxic potential of a cationic lipid-based gene delivery nanosystem in human alveolar epithelial a549 cells. *Toxicol Mech Methods* **18**, 369–78 (2008).

19. Zhao, F. *et al.* Cellular Uptake, Intracellular Trafficking, and Cytotoxicity of Nanomaterials. *Small* **7**, 1322–1337 (2011).

20. Braydich-Stolle, L., Hussain, S., Schlager, J. J. & Hofmann, M. C. In vitro cytotoxicity of nanoparticles in mammalian germline stem cells. *Toxicol. Sci.* **88**, 412–419 (2005).

21. Soenen, S. J. H. & De Cuyper, M. Assessing iron oxide nanoparticle toxicity in vitro: current status and future prospects. *Nanomedicine* **5**, 1261–1275 (2010).

22. Solanki, A., Kim, J. D. & Lee, K. B. Nanotechnology for regenerative medicine: nanomaterials for stem cell imaging. *Nanomedicine* **3**, 567–578 (2008).

23. Yoo, J. W., Irvine, D. J., Discher, D. E. & Mitragotri, S. Bio-inspired, bioengineered and biomimetic drug delivery carriers. *Nature Rev. Drug Discov.* **10**, 521–535 (2011).

24. Bettinger, C. J., Langer, R. & Borenstein, J. T. Engineering substrate topography at the micro- and nanoscale to control cell function. *Angew Chem Int Ed Engl* **48**, 5406–15 (2009).

25. Yim, E. K., Darling, E. M., Kulangara, K., Guilak, F. & Leong, K. W. Nanotopography-induced changes in focal adhesions, cytoskeletal organization, and mechanical properties of human mesenchymal stem cells. *Biomaterials* **31**, 1299–306 (2010).

26. Adler, A. F. & Leong, K. W. Emerging links between surface nanotechnology and endocytosis: impact on nonviral gene delivery. *Nano Today* **5**, 553–569 (2010).

27. Teo, B. K. *et al.* The effect of micro and nanotopography on endocytosis in drug and gene delivery systems. *Biomaterials* **32**, 9866–75 (2011).

28. Saha, K. *et al.* Substrate modulus directs neural stem cell behavior. *Biophys J* **95**, 4426–38 (2008).

29. Jung, J. *et al.* Selective Inhibition of Human Brain Tumor Cells through Multifunctional Quantum-Dot-Based siRNA Delivery. *Angewandte Chemie International Edition* **49**, 103–107 (2010).

30. Moe, A. A. *et al.* Microarray with micro- and nano-topographies enables identification of the optimal topography for directing the differentiation of primary murine neural progenitor cells. *Small* **8**, 3050–61 (2012).

31. Dhara, S. K., Majumder, A., Dodla, M. C. & Stice, S. L. Nonviral gene delivery in neural progenitors derived from human pluripotent stem cells. *Methods Mol Biol* **767**, 343–54 (2011).

32. Myung, S. *et al.* Graphene-Encapsulated Nanoparticle-Based Biosensor for the Selective Detection of Cancer Biomarkers. *Adv. Mater.* **23**, 2221–+ (2011).

33. Dhaliwal, A., Lam, J., Maldonado, M., Lin, C. & Segura, T. Extracellular matrix modulates non-viral gene transfer to mouse mesenchymal stem cells. *Soft Matter* **8**, 1451–1459 (2012).

34. Khormaee, S., Ali, O. A., Chodosh, J. & Mooney, D. J. Optimizing siRNA efficacy through alteration in the target cell-adhesion substrate interaction. *J Biomed Mater Res A* **100**, 2637–43 (2012).

35. Reddi, A. H. Role of morphogenetic proteins in skeletal tissue engineering and regeneration. *Nature Biotech.* **16**, 247–252 (1998).

36. Kalluri, R. Basement membranes: Structure, assembly and role in tumour angiogenesis. *Nature Rev. Cancer* **3**, 422–433 (2003).

37. Bengali, Z., Rea, J. C. & Shea, L. D. Gene expression and internalization following vector adsorption to immobilized proteins: dependence on protein identity and density. *J Gene Med* **9**, 668–78 (2007).

38. Kong, H. J., Hsiong, S. & Mooney, D. J. Nanoscale cell adhesion ligand presentation regulates nonviral gene delivery and expression. *Nano Lett* **7**, 161–6 (2007).

39. Pelkmans, L., Burli, T., Zerial, M. & Helenius, A. Caveolin-stabilized membrane domains as multifunctional transport and sorting devices in endocytic membrane traffic. *Cell* **118**, 767–780 (2004).

40. Stolt, C. C. *et al.* The Sox9 transcription factor determines glial fate choice in the developing spinal cord. *Gene. Dev.* **17**, 1677–1689 (2003).

41. Cheng, L. C., Pastrana, E., Tavazoie, M. & Doetsch, F. miR-124 regulates adult neurogenesis in the subventricular zone stem cell niche. *Nature Neurosci.* **12**, 399–408 (2009).

42. Makeyev, E. V., Zhang, J. W., Carrasco, M. A. & Maniatis, T. The MicroRNA miR-124 promotes neuronal differentiation by triggering brain-specific alternative Pre-mRNA splicing. *Mol. Cell* **27**, 435–448 (2007).

43. Sato, T., Ishii, T. & Okahata, Y. In vitro gene delivery mediated by chitosan. Effect of pH, serum, and molecular mass of chitosan on the transfection efficiency. *Biomaterials* **22**, 2075–2080 (2001).

44. Segura, T., Volk, M. J. & Shea, L. D. Substrate-mediated DNA delivery: role of the cationic polymer structure and extent of modification. *J Control Release* **93**, 69–84 (2003).

45. Bengali, Z. *et al.* Gene delivery through cell culture substrate adsorbed DNA complexes. *Biotechnol Bioeng* **90**, 290–302 (2005).

46. Mehrotra, S., Lee, I. & Chan, C. Multilayer mediated forward and patterned siRNA transfection using linear-PEI at extended N/P ratios. *Acta Biomater* **5**, 1474–88 (2009).

47. Oyane, A., Tsurushima, H. & Ito, A. Highly efficient gene transfer system using a laminin-DNA-apatite composite layer. *J Gene Med* **12**, 194–206 (2010).

48. Kam, K. R. *et al.* Nanostructure-Mediated Transport of Biologics across Epithelial Tissue: Enhancing Permeability via Nanotopography. *Nano Lett* **13**, 164–71 (2013).

49. Park, S., Kim, Y. S., Kim, W. B. & Jon, S. Carbon nanosyringe array as a platform for intracellular delivery. *Nano Lett* **9**, 1325–9 (2009).

50. Shalek, A. K. *et al.* Nanowire-Mediated Delivery Enables Functional Interrogation of Primary Immune Cells: Application to the Analysis of Chronic Lymphocytic Leukemia. *Nano Letters* **12**, 6498–6504 (2012).

51. Shalek, A. K. *et al.* Vertical silicon nanowires as a universal platform for delivering biomolecules into living cells. *Proc Natl Acad Sci U S A* **107**, 1870–5 (2010).

## Acknowledgments

## Author contributions

A.S. initiated the original idea. A.S. and S.S. performed the research. P.T.Y. carried out the PCR analysis. K.-B.L., A.S. and S.S. designed the experiments, analyzed the data and wrote the manuscript together. All the authors discussed the results and reviewed the manuscript.

## Additional information

**How to cite this article:** Solanki, A., Shah, S., Yin, P.T. & Lee, K.-B. Nanotopography-mediated Reverse Uptake for siRNA Delivery into Neural Stem Cells to Enhance Neuronal Differentiation. *Sci. Rep.* **3**, 1553; DOI:10.1038/srep01553 (2013).